Effect of Mg content in Ag/$Zn_{1-X}Mg_XO$/Cu structure for bipolar resistive switching performances

Dibyaranjan Mallick, Rahul Barman, Kirandeep Singh, Ravi Prakash and Davinder Kaur*

Functional Nanomaterials Research Lab, Department of Physics and Centre for Nanotechnology, Indian Institute of Technology Roorkee, Roorkee, Uttarakhand-247667, India

*Corresponding author

DOI: 10.5185/amlett.2018.6952
www.vbripress.com/aml

Abstract

In this study, the bipolar resistive switching behavior of Pulsed Laser Deposited $Zn_{1-x}Mg_xO$ (x= 0, 0.1) thin films in Ag/$Zn_{1-X}Mg_xO$/Cu structure has been investigated. The XRD pattern of $Zn_{1-X}Mg_xO$ exhibits the presence of (002) and (103) reflection. The cross sectional field emission scanning electron microscopy (FE-SEM) studies were further carried out to examine the thickness of the film. In order to analyze the bipolar resistive switching behavior of the $Zn_{1-x}Mg_xO$ thin films, an I-V measurement was performed at room temperature. The memory cell Ag/$Zn_{0.9}Mg_{0.1}O$/Cu exhibits set voltage (ON state) at 2.57V and reset voltage (OFF state) at -3.15 V, excellent OFF to ON resistance ratio (~10^5) for 200 DC sweep cycles and exhibits good retention (>10^3 s). The physical mechanism responsible for exhibiting switching behavior in the $Zn_{1-x}Mg_xO$ thin films was explained by formation and rupture of the nano-scale conduction filament due to Oxygen vacancies. Ohmic conduction and Poole-Frenkel emission are responsible for current conduction in Low Resistance State (LRS) and High Resistance State (HRS) regions respectively. Enhanced switching behavior is observed by substitution of Mg in ZnO thin film. Nonvolatile two resistance states of the $Zn_{1-X}Mg_xO$ thin film could prove useful in future power efficient memory devices. Copyright © 2018 VBRI Press.

Keywords: Resistive switching, oxygen vacancy, compliance current, transition metal oxide, poole-frenkel.

Introduction

Recent time, flash memory is the most widely used non-volatile memory device for solid state disk drives and other storage media. Its operation mechanism is based on charge storage. Thus it is facing technological limits such as packaging density and access speed. Recently it has been demonstrated that Metal-Insulator-Metal (MIM) structure shows nonvolatile memory effect. On applying a voltage pulse to MIM structure, if at least two resistance states i.e. High resistance state (HRS) and Low Resistance State (LRS) is found, then memory effect is realized and it can be used as nonvolatile Resistive Random Access memory (ReRAM). Migration of Oxygen voids or vacancies in oxide layer is the mechanism for occurrence of switching phenomenon in ReRAM devices. During the forming process these vacancies are created and resulting in the formation of nanoscale conductive filament (CF). Formation of filament due to Oxygen vacancies composed conductive channels enable the device to act as a switch. ReRAM reflecting advantages like high speed, low voltage operation, ease of deposition by conventional systems, good compatibility with complementary metal-oxide semiconductor (CMOS) process, excellent scalability and simple memory cell structure favorable for increased integration density. Thus it has great application potential for future nonvolatile memory.

The resistive switching behavior have been observed in various materials including transition metal oxides (TMO) specially binary metal oxide thin films such as TiO_2 [1], NiO [2], ZrO_2 [3], ZnO[4] and perovskite oxides [**5, 6**]. Among those materials, TMO is preferred as it is compatible with present semiconductor technology [**7**]. Various studies already demonstrated the enhancement of resistance switching performances using doping method. It is observed that the doping of the materials such as Mn [**8**], Li [**9**] and Ti [**10**] in ZnO enhanced the resistive switching properties.

In this work, the effect of Mg substitution on resistive switching performance in ZnO thin film and the corresponding switching mechanism has been studied. A comparative study of effect of Mg doping in ZnO is observed for improvement of various resistive switching properties. With the increase in Mg contents in $Zn_{1-x}Mg_xO$ thin film results a high OFF/ON resistance in the range of (10^4~10^5) and enhanced window margin (~10^4) improves the signal-to-noise ratio of memory devices. A wide voltage gap (~5.5V) between the set and reset voltage distribution minimizes the reset failure problems.

Experimental

The targets of pure ZnO and 10% Mg doped ZnO in powder form for syntheses of thin films were prepared by conventional solid state reaction method. Both the powders were calcinated at 400°C for 6 hours, after grinding for 7-8 hours. These calcinated powders were transformed into palate of diameter 16 mm by hydraulic pressure. The palates of ZnO, Mg-doped ZnO ($Zn_{0.9}Mg_{0.1}O$) were sintered at 600°C and 1000°C for 8 hours and 12 hours respectively using ceramic sintering process. For deposition of films initially the Si Substrates were cleaned thoroughly in an ultrasonic bath with distilled water mixed with trichloroethylene in 4:1 ratio. In order to fabricate MIM structure of $Ag/Zn_{1-x}Mg_xO/Cu$, the Cu bottom electrode layer and $Zn_{1-x}Mg_xO$ thin film deposited by the Sputtering and PLD respectively. The Ag top electrode of 300 µm diameter, synthesized by sputtering after applying a shadow mask on the $Zn_{1-x}Mg_xO/Cu$. Before deposition, chamber was vacuumed to a base pressure of the order of 4×10^{-6} torr. To avoid thickness gradient across the film, the typical size of the substrate was selected as 5×5 mm^2 which was smaller than the confined PLD plume. For the deposition of $Zn_{1-x}Mg_xO$ layer on the Cu coated Si substrate, Oxygen pressure and the substrate to target distance were maintained at 20 mtorr, and 4 cm respectively. The deposition was done at room temperature and the laser energy density at the target surface was maintained at 1.9 J/cm^2. The laser beam of 300 mJ energy and 5 HZ repetition rate was focused onto the targets. The schematic of the MIM structure is shown in inset of **Fig.1**.

The crystallinity and orientation of the films were characterized using a Bruker AXS – D8 advanced X-ray diffractometer of Cu Kα (1.54 Å) radiation in θ-2θ geometry at a scan speed 1°/min. The cross sectional interface of the thin films were investigated by Field Emission Scanning Electron Microscope (FE-SEM). The resistive switching behaviors of the films were studied at room temperature by Keithley 4200 semiconductor characterization system (SCS) Analyzer.

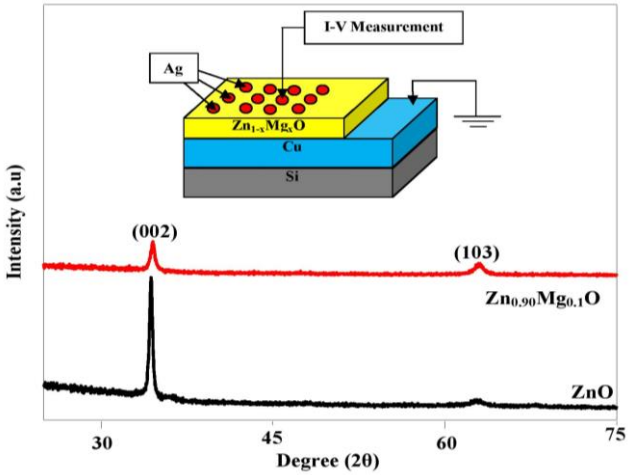

Fig. 1 X-ray diffraction pattern of ZnO and $Zn_{0.9}Mg_{0.1}O$ films. The inset shows schematic structure of the $Ag/Zn_{1-x}Mg_xO/Cu$ ReRAM memory cell.

Results and discussion

Fig.1 shows the X-ray diffraction pattern of ZnO and $Zn_{0.9}Mg_{0.1}O$ thin films, which revealed the presence of (103) and dominant (002) orientation. As the Mg content in $Zn_{1-x}Mg_xO$ increases, the peaks slightly shift towards high diffraction angle is observed. This shifting could be due to Mg atoms assimilate into ZnO lattice [**13**]. **Fig. 2 (a)** and **(b)** shows the FE-SEM image of ZnO and $Zn_{0.9}Mg_{0.1}O$ thin film respectively which indicates that the thin film surface is dense, smooth and having uniformly distributed grains. Cross sectional FE-SEM **(Fig. 2 (c))** conforms the film thickness is 145 nm thick and having a good quality interface.

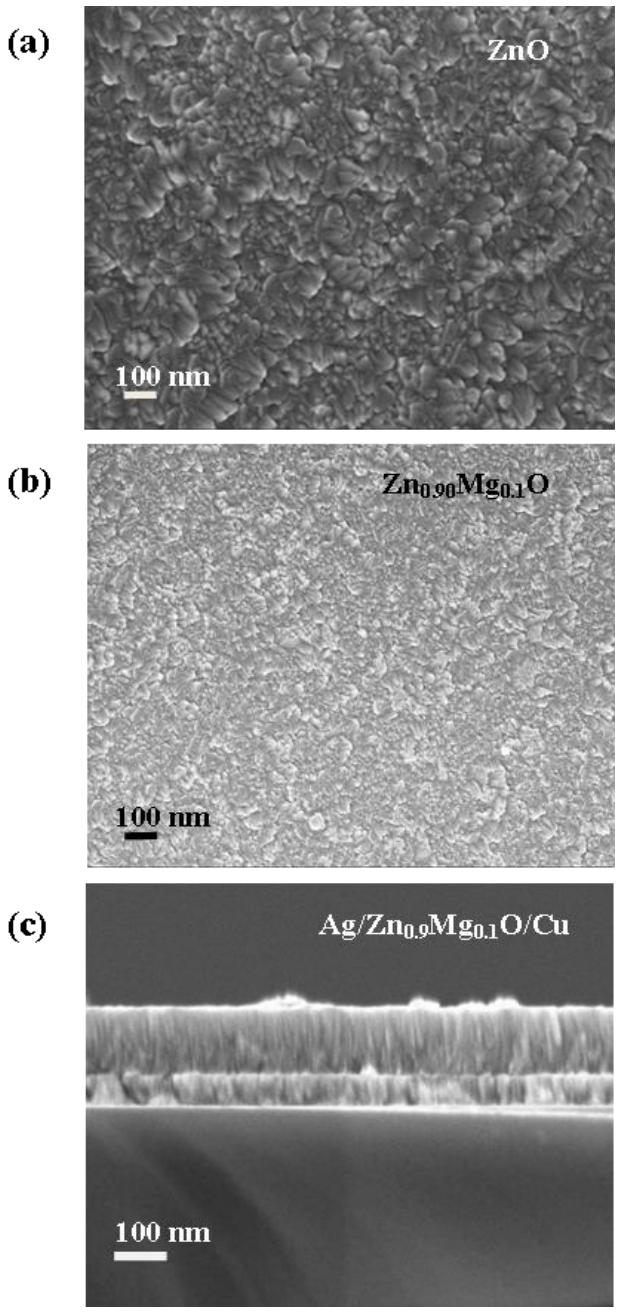

Fig. 2 (a), (b) shows FE-SEM image of ZnO and $Zn_{0.9}Mg_{0.1}O$ thin films respectively and (c) Cross sectional FE-SEM image of $Zn_{0.9}Mg_{0.1}O/Cu/Si$ film.

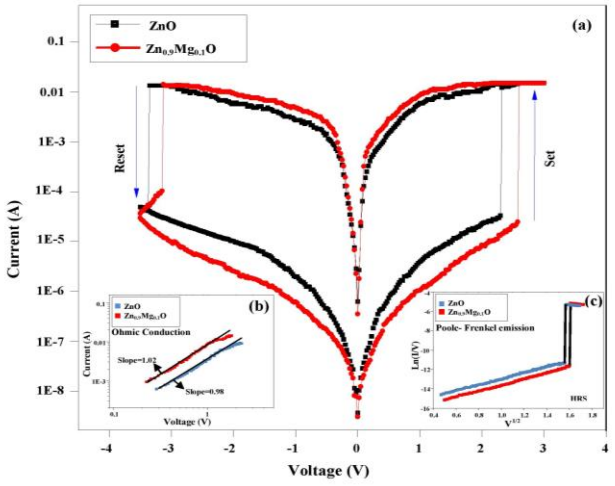

Fig. 3 (a) Typical bipolar resistive switching characteristics for $Ag/Zn_{1-x}Mg_xO/Cu$ memory cell for a DC voltage sweep (0V→3.5V→0V→-3.5V→0V). Conduction mechanism of $Ag/Zn_{1-x}Mg_xO/Cu$ thin film (b) Ohmic conduction in LRS region and (c) Poole-Frenkel emission in HRS region.

To examine the resistive switching behavior of $Ag/Zn_{1-x}Mg_xO/Cu$ thin films, a DC sweeping sequence of 0V → +3.5V → 0V → -3.5V →0V was applied by SCS setup. Biasing voltage was applied on the Ag top electrode while the Cu bottom electrode was kept grounded. A compliance current (CC) of about 15 mA was set in order to prevent the film from permanent breakdown. It was found that the films were initially in the HRS. **Fig. 3 (a)** shows a typical bipolar current voltage (I-V) characteristics for the $Ag/Zn_{1-x}Mg_xO/Cu$ structure for x= 0 and 0.1. When a positive voltage pulse (0V → +3.5 V) was applied to the top electrode of Ag/ZnO/Cu in HRS, there was a linear increase in current in log-linear scale is observed as shown in **Fig. 3(a).** At about +2.32 V (set voltage V_{set}) the current abruptly increase and the film comes into ON state (LRS). This ON state occurred due to filament forming process. When a negative voltage pulse (0V → -3.5V) was applied to the top electrode of the memory cell in LRS, at about -3.36V (reset voltage V_{reset}) the film switches back to HRS (off state). This process is called as reset process.

To investigate the effect of Mg substitution in ZnO on resistive switching behavior, Mg is doped up to 10% in ZnO ($Zn_{0.9}Mg_{0.1}O$). An I-V measurement is repeated as performed for Ag/ZnO/Cu. The observed V_{set} for $Ag/Zn_{0.9}Mg_{0.1}O/Cu$ is +2.57 V which is slightly larger than V_{set} for Ag/ZnO/Cu and V_{reset} is around -3.15 V as shown in **Fig. 3(a).**

The current conduction mechanism of $Ag/Zn_{1-x}Mg_xO/Cu$ memory cell has been understood by replotting the I-V curves in both LRS and HRS regions. **Fig. 3(b)** shows the plot between log (I) Vs log (V) for the films in LRS region. In the voltage region of ($V<V_{set}$) of the ON-state exhibits a linear increase in current with a slope of 0.98 and 1.02 is detected for ZnO and $Zn_{0.9}Mg_{0.1}O$ films respectively. It confirms the conduction mechanism in the LRS region is dominated by ohmic behavior [**11**]. In the HRS region the current conduction mechanism can be explained by Poole-Frenkel (PF) emission theory [12] can be characterized by equation (1).

$$\ln\left(\frac{I}{V}\right) \approx \left[\left(\frac{q^3}{\pi d \varepsilon_0 \varepsilon_r}\right)^{\frac{1}{2}}\right]\frac{V^{\frac{1}{2}}}{K_B T} \quad (1)$$

here *d* is the thickness of the film, q is the electric charge, ε_0 is the permittivity of free space, ε_r is the dynamic dielectric constant, K_B is Boltzmann's constant and T is the Kelvin temperature. According to the equation (1), the dominant current conduction mechanism can be interpreted in terms of the relation between ln (I/V) Vs $V^{1/2}$. **Fig. 3(c)** shows replotting of experimental data can be fitted Poole-Frenkel emission over the low voltage region ($V<V_{set}$) in the HRS region. So the carrier trapping and detrapping of Poole-Frenkel emission theory is considered as the main mechanism in HRS.

A filamentary model is proposed to explain the physical mechanism behind the resistive switching behavior of $Zn_{1-x}Mg_xO$ thin film. From previous studies, it is inevitable that some defects like interstitial atoms and Oxygen vacancies are present in $Zn_{1-x}Mg_xO$ thin film [**13**]. Oxygen void defects are intrinsic crystal defects such as Oxygen vacancies. This type of defect is formed when an Oxygen atom is missing from a position that ought to be filled in the crystal. Oxygen vacancies creation and recombination is the dominant mechanism for RS behavior. The schematic diagram in **Fig. 4 (a)** depicts the formation and rupture of filament due to Oxygen vacancies. During the set process, Oxygen atoms are removed from the switching layer and Oxygen vacancies are created in the switching layer [**2, 14**]. Oxygen ions are drifted and are stored at the Ag interface forming an Oxygen reservoir. Thus a conducting filament is formed between the top and bottom electrode which results LRS. As a read pulse is applied, the carriers transport through the filamentary path, exhibiting ohmic I-V behavior. The film remains on LRS until the filament ruptures. During the reset pulse, Oxygen ions drift from the interface back to the switching layer and recombine with the Oxygen vacancies created during set process. This causes rupture of conducting filaments near the Ag interface and the resistance state of the device changes to the HRS.

The endurance property is measured by applying 1V of read pulse to ZnO and $Zn_{0.9}Mg_{0.1}O$ films before and after the forming process up to 200 cycles. **Fig. 4 (b)** shows the OFF and ON resistance values in HRS and LRS region respectively for both the films. It is observed that the minimum value of resistance ratio (ratio of OFF to ON resistance $R_{H/L}$) for ZnO film is 125. However the $R_{H/L}$ value for $Zn_{0.9}Mg_{0.1}O$ film is approximately in order of 10^5 which is an excellent value in comparison with undoped ZnO film. The memory window (w) [**15**] of a memory cell can be defined as

$$w = (R_{OFF}-R_{ON})/R_{ON} \sim R_{OFF}/R_{ON} \quad (2)$$

here R_{OFF}, R_{ON} are the resistance of the OFF and ON state, respectively. For ZnO thin film the memory window

distributes between 136 and 1225. However for $Zn_{0.9}Mg_{0.1}O$ film the memory window distributes between 7×10^3 and 4×10^5. The memory window margin (w_m) [**15**] can be defined as

$$w_m = (R_{OFF}^{min} - R_{ON}^{max})/\, R_{ON}^{max} \sim R_{OFF}^{min}/R_{ON}^{max} \qquad (3)$$

here R_{OFF}^{min} is the minimum resistance of the OFF state and R_{ON}^{max} is the maximum resistance of the ON state measured within the 200 cycles. The memory window margin for ZnO film is 3×10^3 where as for $Zn_{0.9}Mg_{0.1}O$ is larger than 4×10^4. This increase in $R_{H/L}$ ratio and memory window improves the signal to noise ratio for memrister application. In HRS region the resistivity of $Zn_{0.9}Mg_{0.1}O$ film is higher compared to ZnO thin film. In ZnO, the presences of interstitial Zinc atoms create donor levels. Carrier electrons excited thermally from the donor level resulting ZnO an n-type semiconductor. When ZnO is doped with Mg, interstitial metal atoms and Oxygen void defects could be depressed, because formation energy of Mg-doped ZnO increases [**9**]. On other hand, Mg doping in ZnO results increase in band gap. Thus the decrease in the defects and increase in band gap causes increase in resistivity of $Zn_{0.9}Mg_{0.1}O$ thin film in HRS region. However in LRS region a conducting filament is formed for both the films resulting no difference in resistivity. It is observed that, at the initial cycle testing the OFF resistance value is high and unstable and after some switching cycles (after 150 cycles) become relatively stable. The ON resistance values at the LRS region are noticeably steady within 200 switching cycles. This decrease in the OFF resistance in the thin film can be explained by Joule heating effect [**16**]. Kim *et al.* reported that additional filament could be formed nearby the first filament by local Joule heating due to high current density [**17**]. These enhance the filament formation and as a result conductivity increases. This increase in conductivity increases the current in the OFF state and thus results in decrease the OFF state resistance. In the ON state the semiconductor-metal junction is forward biased. So there is relatively small effect of temperature and filament formation. Hence no change in resistance is observed in the ON state.

Fig. 4 (c) shows the distribution of set and reset voltage for both films by application of 200 DC pulses. It is observed that for $Ag/Zn_{0.9}Mg_{0.1}O/Cu$ structure the distribution of V_{set} is 0.42 V and V_{reset} is 0.27V while for Ag/ZnO/Cu film the distribution of V_{set} and V_{reset} is 0.45V and 0.22V respectively. This large variation in V_{set} occurrence can be explained as according to the conducting filament model. During the formation and rapture process of a filament, the development of a filament should be irregular than the destruction of an existing filament. Large voltage gap (~5.5V) results no RESET failure in the 200 measured cycles. **Fig. 4 (d)** shows the data retention performance of Ag/ZnO/Cu and $Ag/Zn_{0.9}Mg_{0.1}O/Cu$ structure at room temperature. The OFF and ON resistance in LRS and HRS regions were measured for more than 2×10^3 s at 1 V in sampling mode. Good retention property and very good endurance property for $Zn_{0.9}Mg_{0.1}O$ thin film is observed which is listed in **Table 1**. This table clearly signified that the values of V_{set} and V_{reset} in $Ag/Zn_{0.9}Mg_{0.1}O/Cu$ are smaller as compared to Ag/ZnO/Cu. However minimum $R_{H/L}$ and memory window margin (W_m) values are larger.

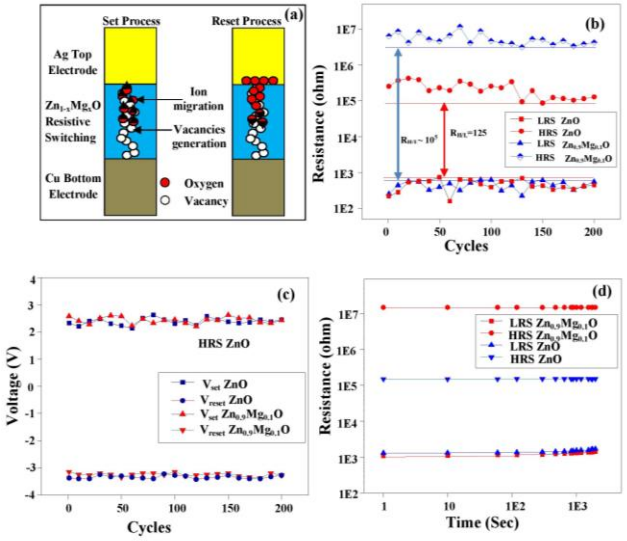

Fig. 4. (a) Schematic diagram of the switching mechanism of $Ag/Zn_{1-x}Mg_xO/Cu$ memory cell, (b) Endurance performance of $Ag/Zn_{1-x}Mg_xO/Cu$ thin films for 200 switching cycles at 1V read pulse, (c) Set and reset voltage distribution of both films and (d) Data retention property of both memory cells.

Table 1. Values of V_{set} and V_{reset} in $Ag/Zn_{0.9}Mg_{0.1}O/Cu$ and Ag/ZnO/Cu.

Device	Distri-bution of V_{set}	Distri-bution of V_{reset}	Minimun $R_{H/L}$	Memory window Margin (W_m)	$R_{H/L}$ (after 200 cycles)	$R_{H/L}$ (after 2×10^3 sec)
Ag/ZnO/Cu	0.43	0.27	125	3×10^3	~110	~80
$Ag/Zn_{0.9}Mg_{0.1}O/Cu$	0.42	0.22	$\sim10^5$	4×10^4	$\sim10^4$	$\sim\sim10^4$

Conclusion

In summary $Zn_xMg_{1-x}O$ thin films were prepared on Cu coated Si substrate by PLD technique having good crystalline quality with preferred (002) orientation. Formation and rupture of conductive filament via migration of Oxygen ions and vacancies are the main cause for resistive switching behavior in $Ag/Zn_{1-x}Mg_xO/Cu$. The dominant conduction mechanisms of LRS and HRS are ohmic conduction behavior and Poole-Frenkel emission respectively. On comparison the resistive switching performance of $Mg_{0.1}Zn_{0.9}O$ film with ZnO film, we found that as the concentration of Mg in ZnO is increased, the resistance ratio between HRS and LRS improves from the order of $\sim10^2$ to the order of $\sim10^5$, although the set voltage slightly increases after doping. In addition narrow set/reset voltage distribution, high resistance ratio, good retention property and very good endurance properties observed on $Zn_{0.9}Mg_{0.1}O$ thin film. Thus $Ag/Zn_{0.9}Mg_{0.1}O/Cu$ device can be used as a highly efficient ReRAM device.

Acknowledgements

The financial support provided by the Defense Research and Development Organization (DRDO), India under ER and IPR with Reference No. ERIP/ER/ 1100406/M/01/1439 are highly acknowledged. Author Dibyaranjan Mallick also acknowledged financial support from the Ministry of Human Resource Development (MHRD), India.

References

1. Kim, K. M.; Choi, B. J.; Shin, Y. C.; Choi, S.; Huang, C. S.; *Appl. Phys. Lett.*, **2007,** 91, 012907. **DOI**: 10.1063/1.2749846
2. Son, J. Y.; Shin, Y. H.; *Appl. Phys. Lett*., **2008,** 92, 222106. **DOI**: 10.1063/1.2931087
3. Liu, Q.; Guan, W.; Long, S.; Jia,R.; Liu, M.; Chen, J.; *Appl. Phys. Lett*., **2008,** 92, 012117. **DOI**: 10.1063/1.2832660
4. Chang, W.Y.; Lai, Y.C.; Wu, T.B.; Wang, S.F.; Chen, F.; Tsai, M.J.; *Appl. Phys. Lett.*, **2008,** 92, 022110. **DOI**: 10.1063/1.2834852
5. Liu, S.Q.; Wu, N.J.; Ignatiev, A.; *Appl. Phys. Lett,*. **2000,** 76, 2749. **DOI**: 10.1063/1.126464
6. Watanabe, Y.; Bednorz, J.G.; Bietsch, A.; Gerber, C.; Widmer, D.; Beck, A.; Wind, S.J.; *Appl. Phys. Lett*., **2001,** 78, 3738. **DOI**: 10.1063/1.1377617
7. Cheng, H. C.; Chen, S. W.; Wu, J. M.; *Thin Solid Films*, **2011,** 519, 6155. **DOI**: 10.1016/j.tsf.2011.04.013
8. Peng, H. Y.; Li, G. P.; Ye, J. Y.; Wei, Z. P.; Zhang, Z.; Wang, D. D.; Xing, G. Z.; Wu, T.; *Appl. Phys. Lett.*, **2010,** 96, 192113. **DOI**: 10.1063/1.3428365
9. Liu, J.; Weng, W.; Ding, W.; Cheng, K.; Du, P.; Shen, G.; Han, G.; *Surf. Coat. Technol.*, **2005,** 198, 274–277. **DOI**: 10.1016/j.surfcoat.2004.10.081
10. Younis, A.; Chu, D.; Li, S.; *Nanoscale Research Letters*, **2013,** 8, 154. **DOI**: 10.1186/1556-276X-8-154
11. Kim, M. J.; Jeon, D. S.; Park, J. H.; Kim, T. G.; *Appl. Phys. Lett*, **2015**, 106, 203101. **DOI**: 10.1063/1.4921349
12. Yeargan, J. R.; Taylor, H. L.; *J. Appl. Phys*., **1968,** 39, 5600. **DOI**: 10.1063/1.1656022
13. Chen, X.; Wu, G.; Bao, D.; *Appl. Phys. Lett.*, **2008,** 93, 093501. **DOI**: 10.1063/1.2978158
14. Chang, W. Y.; Lai, Y. C.; Wu, T. B.; Wang, S. F.; Chen, F.; Tsai, M. J.; *Appl. Phys. Lett*., **2008,** 92, 022110. **DOI**: 10.1063/1.2834852
15. Qi, J.; Ren, J.; Olmedo, M.; Zhan, N.; Liu, J.; *Appl. Phys A*, **2012,** 107, 891. **DOI**: 10.1007/s00339-012-6815-8
16. Uenuma, M.; Ishikawa, Y.; Uraoka, Y.; *Appl. Phys. Lett.*, **2015,** 107, 073503. **DOI**: 10.1063/1.4928661
17. Kim, D. C.; Seo, S.; Ahn, S. E.; Suh, D.-S.; Lee, M. J.; Park, B.-H.; Yoo, I. K.; Baek, I. G.; Kim, H.-J.; Yim, E. K.; Lee, J. E.; Park, S. O.; Kim, H. S.; Chung, U-In.; Moon, J. T.; Ryu, B. I.; *Appl. Phys. Lett.*, **2006,** 88, 202102. **DOI**: 10.1063/1.2204649

